

Profiling the Organic Cation-dependent Degradation of Organolead Halide Perovskite Solar Cells

Teng Zhang,[†] Xiangyue Meng,[†] Yang Bai,[†] Shuang Xiao,[†] Chen Hu,[†] Yinglong Yang,[†] Haining Chen^{†,‡} and Shihe Yang^{*,†}

[†]Nano Science and Technology Program, Department of Chemistry, The Hong Kong University of Science and Technology, Clear Water Bay, Kowloon, Hong Kong

[‡]School of Materials Science and Engineering, Beihang University

*Corresponding Author: chsyang@ust.hk



Figure S1. The daily humidity condition of Hong Kong during our perovskite degradation experiments. The data were downloaded from the Hong Kong Observatory website.

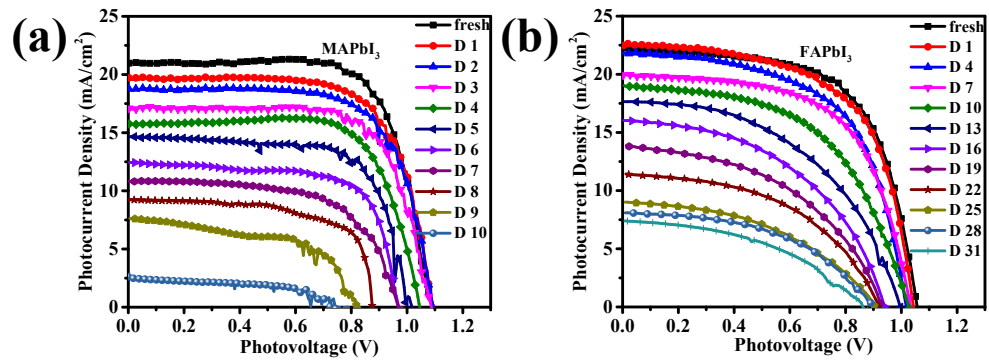


Figure S2. Performance degradation of (a) MAPbI₃ and (b) FAPbI₃ PVSCs devices during the “dark stability” evaluation period of up to 31 days. Here the devices were kept in a dark dry box (~ 20% R.H.) and measured each day under the ambient condition (~ 70% R.H.).

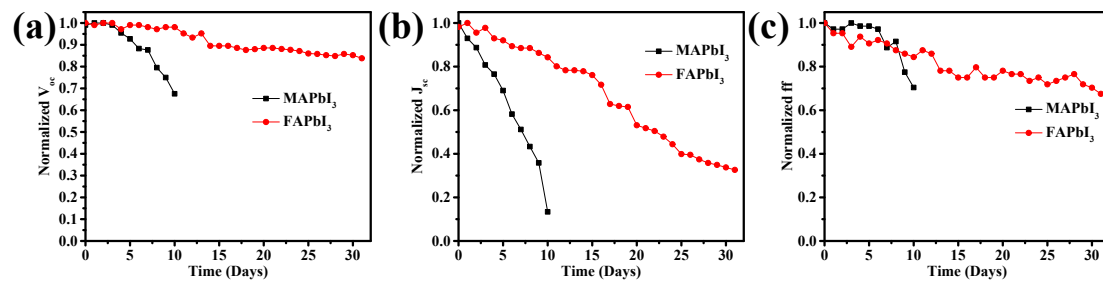


Figure S3. Normalized photovoltaic parameters (a) V_{oc} , (b) J_{sc} and (c) ff variation during the dark stability evaluation period. Here the devices were kept in a dark dry box and measured each day under the ambient condition.

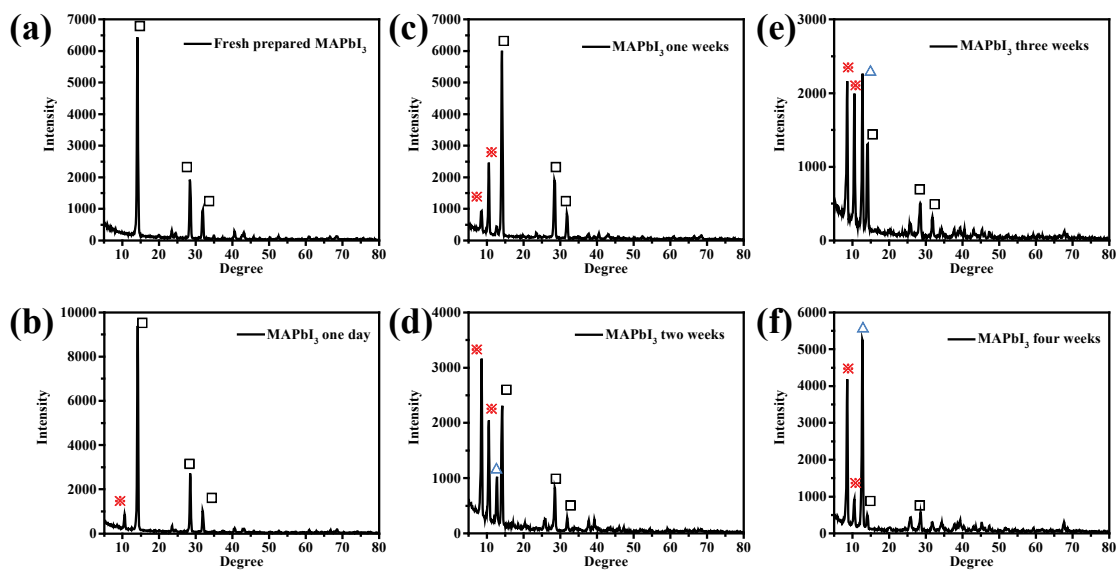


Figure S4. Time-resolved XRD patterns of fresh prepared MAPbI₃ films exposed in the ambient condition for up to approximately a month. The films were measured after 0, 1 day, 1, 2, 3, 4 weeks of exposure to the ambient condition. Peaks labeled with “□” suggest the perovskite phase. The peaks labeled with “✖” correspond to monohydrate CH₃NH₃PbI₃·H₂O phase and “△” to PbI₂ phase.

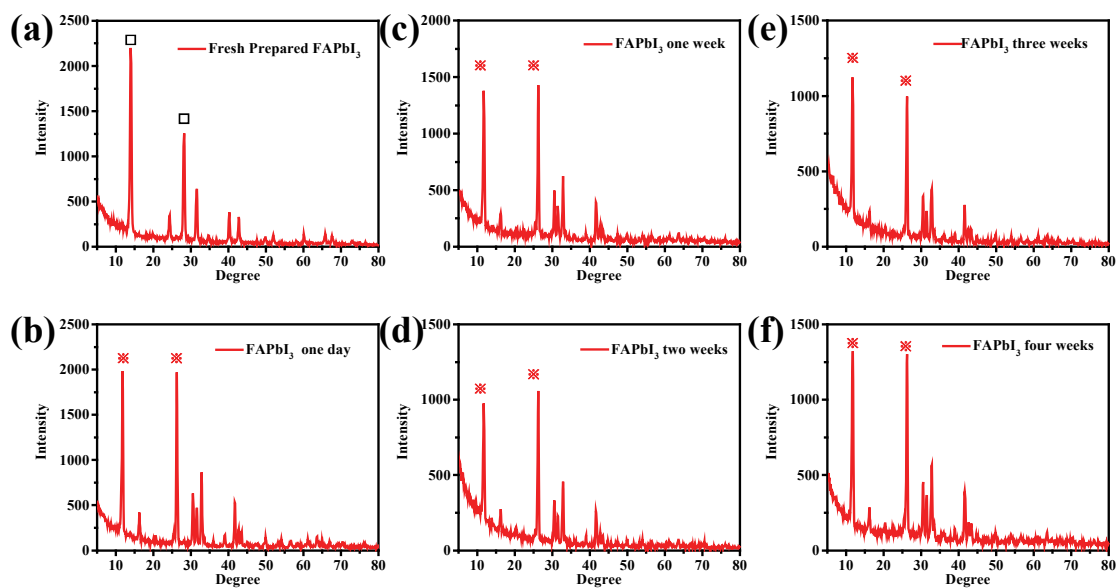


Figure S5. Time-resolved XRD patterns of fresh prepared FAPbI₃ films and those exposed in the ambient condition for up to approximately a month. The films were measured after 0, 1 day, 1, 2, 3, 4 weeks of exposure to the ambient condition. Peaks labeled with “□” suggest the FAPbI₃ high temperature black α phase and “×” the FAPbI₃ low temperature light yellow δ phase.

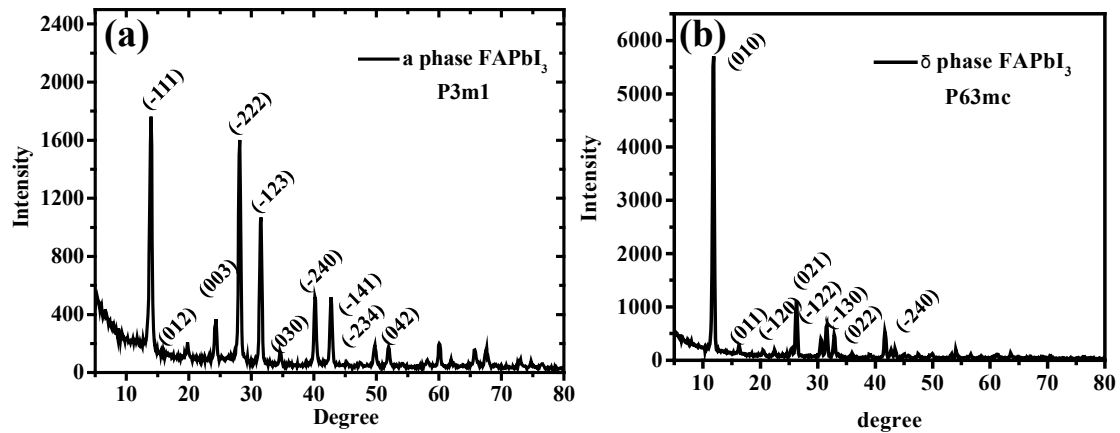


Figure S6. XRD patterns of fresh prepared high temperature black α phase (a) and low temperature δ phase (b) FAPbI₃ perovskite films. The α (δ) phase was annealed at 150 °C (100 °C) for 30 min.

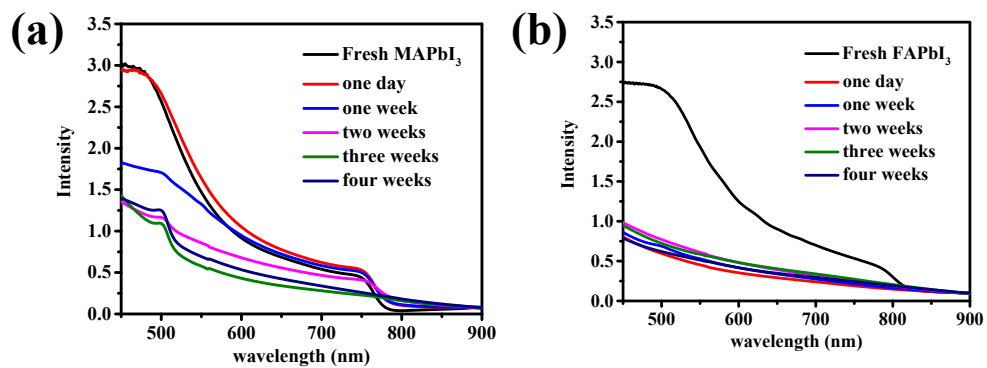


Figure S7. Absorption spectra of MAPbI₃ (e) and FAPbI₃ (f) films after storage in the ambient condition for a period from one day to approximately one month.

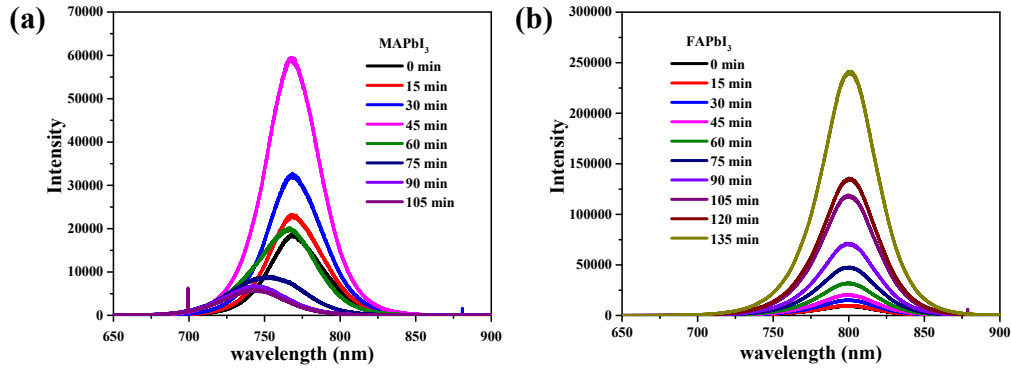


Figure S8. Long term photoluminescence (PL) stability of MAPbI₃ (a) and FAPbI₃ (b) films measured at an interval of 15 min in the ambient condition under continuous laser irradiation. A 512 nm green laser was used ($\sim 0.1 \text{ W/cm}^2$).

We use PL to characterize the photostability of the corresponding perovskite films. Surprisingly, the PL intensity first increased a lot under continuous laser irradiation. Since this laser induced PL enhancement has been reported previously^{1, 2}, in this paper we simply focus on the PL stability instead. The PL intensity of MAPbI₃ films finally dropped after 1 h continuous laser irradiation and the corresponding PL peak shifts from approximately 770 nm to less than 750 nm after 1.5 h continuous laser irradiation (Figure S8 a). This suggests the partial degradation of MAPbI₃ films. As for FAPbI₃, the PL intensity continuous increased even after 2 h irradiation and this PL intensity would not drop until after 4 h continuous irradiation (Figure S8 b, Figure S9). The results suggest the photostability of FAPbI₃ films is far better than that of MAPbI₃. This improved photostability can be explained by a better thermal stability of FAPbI₃ materials than that of MAPbI₃.^{3, 4}

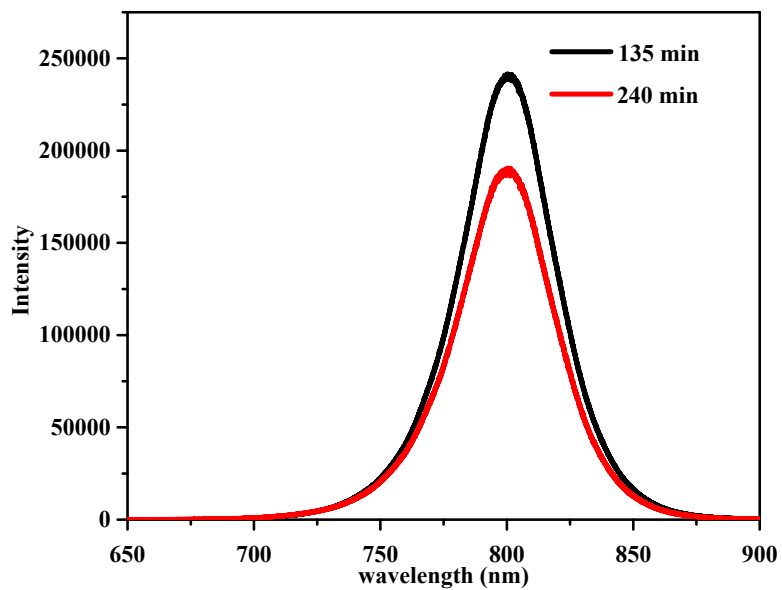


Figure S9. PL spectra of fresh prepared FAPbI₃ films under continuous laser irradiation (514 nm) for 135 min and 240 min, respectively. The PL intensity did not drop until after ~ 4 h of continuous laser irradiation.

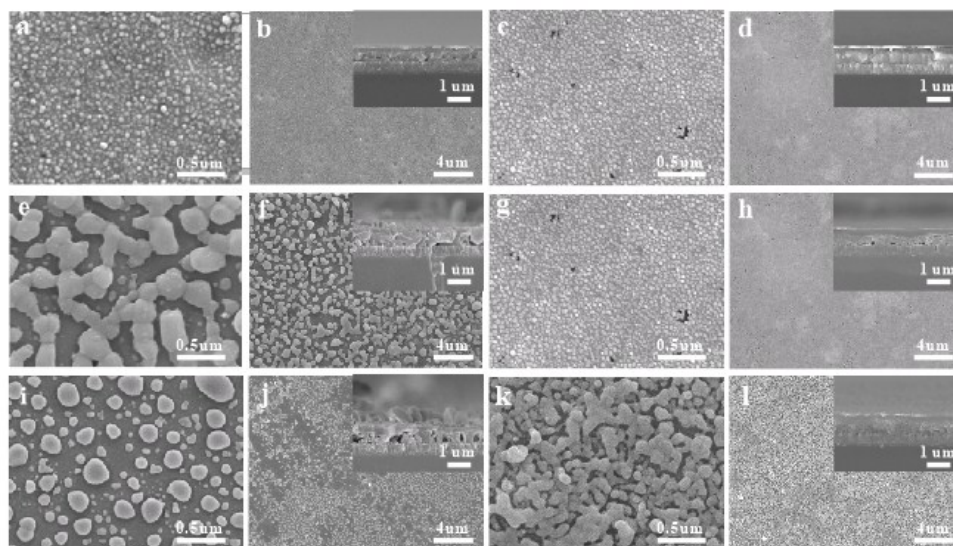


Figure S10. SEM images of PVSC devices (a, b, e, f, i, g: MAPbI₃; c, d, g, h, k, l: FAPbI₃) freshly prepared (a-d), stored in the ambient condition for 3 days (e-h), and stored in the ambient condition for a week (i-l).

To begin with, in fresh prepared PVSCs, the Ag layer is rather smooth consisting of small Ag particles (Figure S10 a-d). However, pin holes can be clearly observed on the surface of Ag back contact (Figure S10 b, d, Figure S11), which act as channels for moisture to diffuse into the devices. A striking feature in MAPbI₃ devices is that, this smooth uniform metal layer turns rough with bare HTM underlayer after exposing to the ambient for a few days. At the same time, small round Ag nanoparticles also aggregate into large crystals (possibly AgI according to our XRD analysis), and this become more and more severe with time. For FAPbI₃ devices, the degradation of Ag back contact also occurs, but much slower than in MAPbI₃ PVSCs. This is consistent with our finding from the XRD analysis (Figure 2), since compared with MAPbI₃ devices, the AgI intensity is much smaller in FAPbI₃ PVSCs.

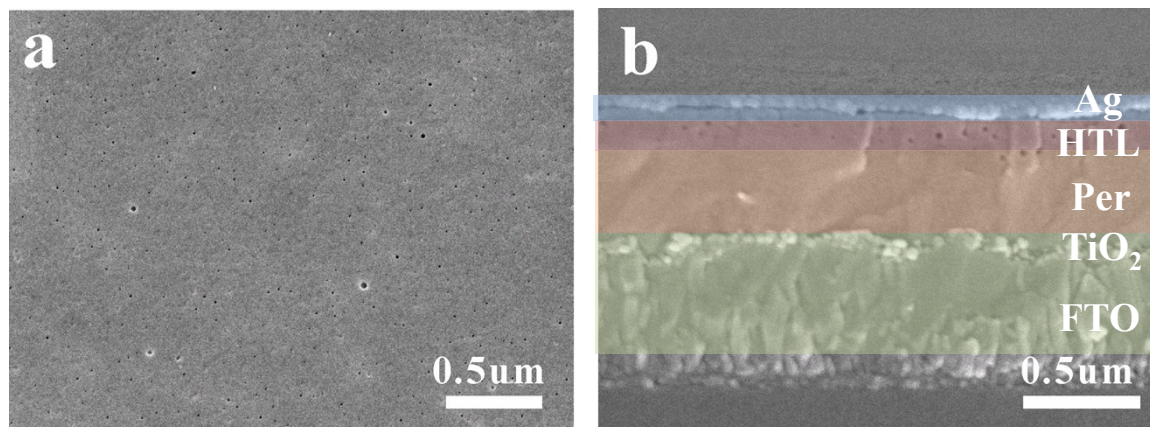


Figure S11. Top-view (a) and cross-view (b) SEM images of fresh prepared FAPbI₃ devices. Here, pin holes can be clearly observed in the top metal contact and the hole transport material layer.

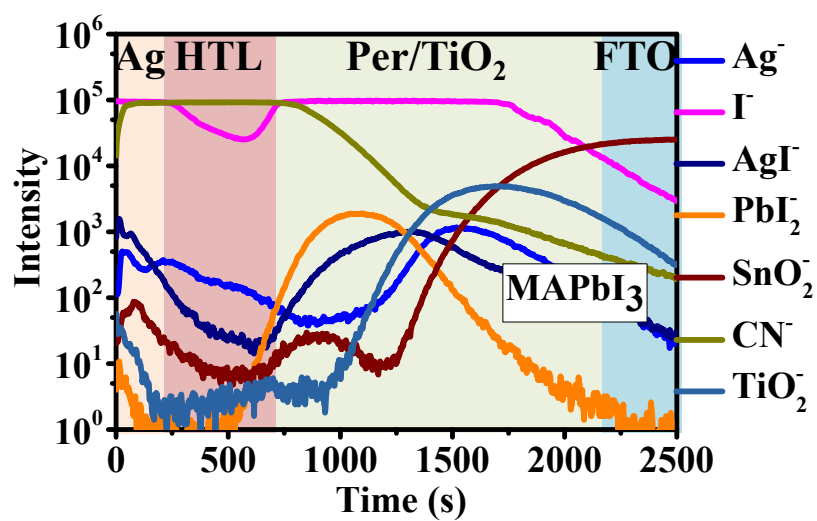


Figure S12. TOF-SIMS profile of a typical degraded MAPbI₃ devices after the operational stability test (5h, 40°C, AM 1.5G continuous illumination). Different element intensities were considered.

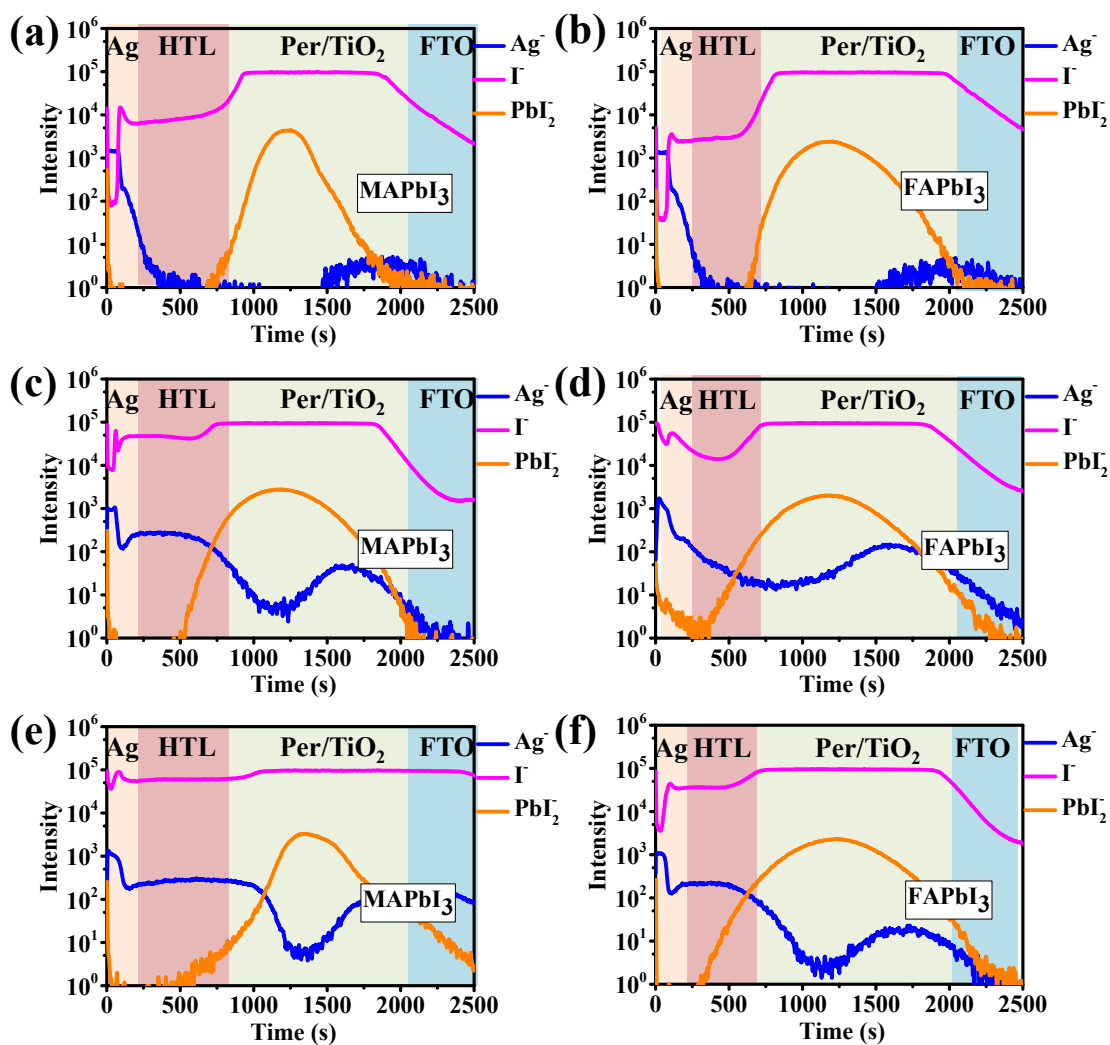


Figure S13. TOF-SIMS profiles of PVSCs (a, c, e, MAPbI₃; b, d, f, FAPbI₃) tracking in the ambient degradation. (a, b) fresh prepared (device exposed outside for 0 days), (c, d) devices exposed to ambient for 3 days, (e, f) devices exposed to ambient for a week.

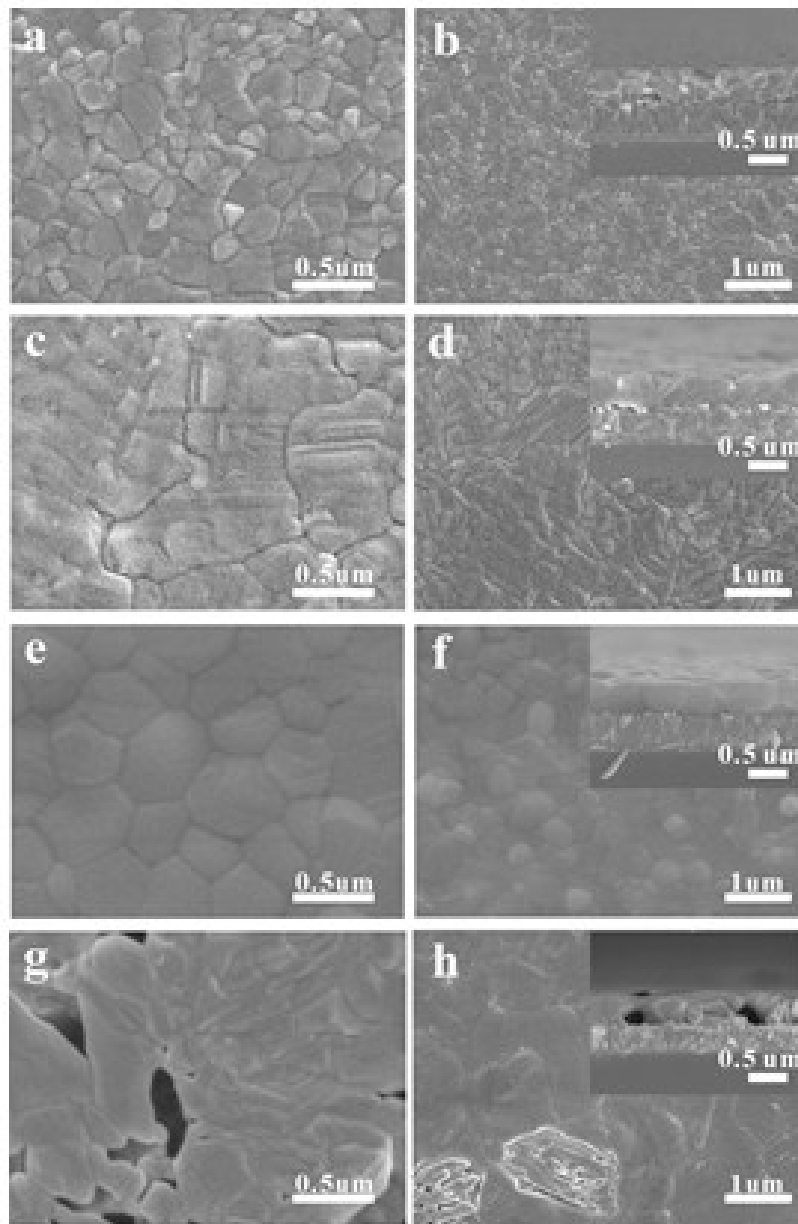


Figure S14. SEM images of fresh prepared MAPbI₃ (a, b), high temperature α phase FAPbI₃(c, d), low temperature δ phase FAPbI₃ (e, f) and α phase FAPbI₃ films exposed outside for a week (g, h). The MAPbI₃ and δ -FAPbI₃ were annealed at 100 °C for 30 min respectively, while the α -FAPbI₃ was annealed at 150 °C for 30 min.

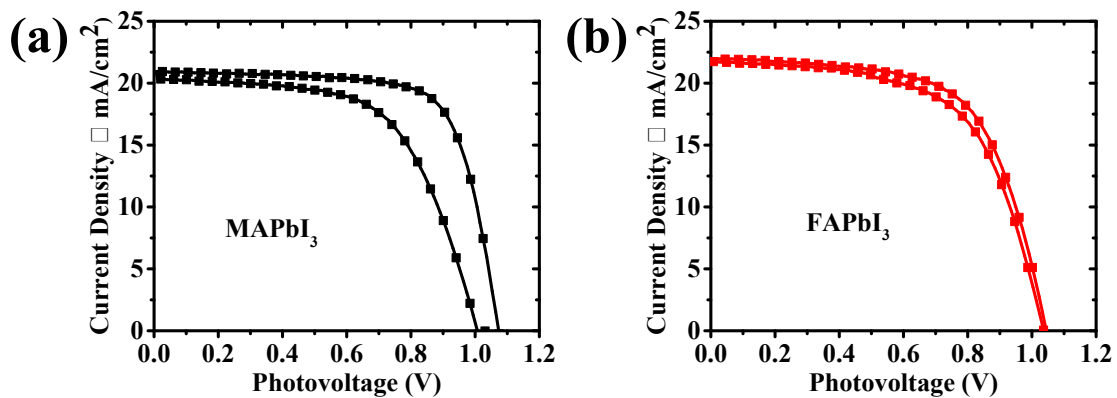


Figure S15: J-V curves of the MAPbI₃ (a) and FAPbI₃ (b) PVSCs under forward scan and reverse scan with a scan rate of 50 mV/s. J-V measurements are performed under AM 1.5G one sun illumination.

Table S1. Photovoltaic parameters obtained at forward scan and reverse scan in different PVSCs with a scan rate of 50 mv/s.

	sweep direction	V_{oc} (V)	J_{sc} (mA/cm ²)	FF	PCE (%)	Hysteresis index (%)
MAPbI ₃	reverse	1.07	20.85	0.73	16.26	26%
	forward	1.01	20.28	0.61	12.49	
FAPbI ₃	reverse	1.04	21.98	0.63	14.46	6.5%
	forward	1.03	21.73	0.61	13.65	

Here the hysteresis index is defined as follows⁵

$$HI = \frac{J_{RS}(0.8V_{oc}) - J_{FS}(0.8V_{oc})}{J_{RS}(0.8V_{oc})} \times 100\%$$

where $J_{RS}(0.8V_{OC})$ and $J_{FS}(0.8V_{OC})$ record the photocurrent density at 80% of the V_{OC} at RS and FS, respectively.

REFERENCE

1. Y. Tian, M. Peter, E. Unger, M. Abdellah, K. Zheng, T. Pullerits, A. Yartsev, V. Sundstrom and I. G. Scheblykin, *Phys. Chem. Chem. Phys.*, 2015, **17**, 24978-24987.
2. H. H. Fang, F. Wang, S. Adjokatse, N. Zhao and M. A. Loi, *Adv. Funct. Mater.*, 2016, **26**, 4653-4659.
3. S. Pang, H. Hu, J. Zhang, S. Lv, Y. Yu, F. Wei, T. Qin, H. Xu, Z. Liu and G. Cui, *Chem. Mater.*, 2014, **26**, 1485–1491.
4. Q. Han, S. H. Bae, P. Sun, Y. T. Hsieh, Y. Yang, Y. S. Rim, H. Zhao, Q. Chen, W. Shi, G. Li and Y. Yang, *Adv. Mater.*, 2016, **28**, 2253–2258.
5. R. S. Sanchez, V. Gonzalez-Pedro, J. W. Lee, N. G. Park, Y. S. Kang, I. Mora-Sero and J. Bisquert, *J. Phys. Chem. Lett.*, 2014, **5**, 2357–2363.